Elastodynamic 2D Green function retrieval from cross-correlation: Canonical inclusion problem

Francisco J. Sánchez-Sesma,[1] Juan A. Pérez-Ruiz,[2] Michel Campillo,[3] and Francisco Luzón[2]

Received 6 April 2006; revised 12 May 2006; accepted 23 May 2006; published 4 July 2006.

[1] It has been demonstrated experimentally and theoretically that cross-correlation at two points subjected to diffuse wavefields leads to the emergence of the Green function. Theoretical derivations imply several ideas of great generality but distinct interpretations exist. One assumes diffuse wavefields generated by multiple scattering. In other there is the assumption of multiple independent, uncorrelated sources giving rise to the phenomenon. Here we study the canonical problem of the retrieval of 2D elastodynamic Green function in an infinite space containing a cylinder inclusion. We illuminate isotropically the space with plane waves. We assume the spectra for both *P* and *SV* uniform and such that the energy ratio $E_S/E_P = (\alpha/\beta)^2$, which is predicted by equipartition theory in 2D. We then show that the Fourier transform of azimuthal average of cross-correlation of motion between two points is proportional to the imaginary part of the corresponding *exact* Green tensor. Some implications are discussed. **Citation:** Sánchez-Sesma, F. J., J. A. Pérez-Ruiz, M. Campillo, and F. Luzón (2006), Elastodynamic 2D Green function retrieval from cross-correlation: Canonical inclusion problem, *Geophys. Res. Lett.*, *33*, L13305, doi:10.1029/2006GL026454.

1. Introduction

[2] The use of correlations of seismic noise and coda waves is becoming a subject of interest. The pioneering approach of *Aki* [1957] is crucial to understand the role of seismic noise. Aki studied descriptions that ranged from single and multiple scattering to radiative transfer ideas that explored to explain coda envelopes [*Sato and Fehler*, 1998].

[3] The elastodynamic Green function has been experimentally recovered from the averaging of cross correlations of the isotropic, diffuse elastic wavefield generated by either multiple scattering or by a large number of sources (such as microseisms) as well [see *Campillo and Paul*, 2003; *Shapiro and Campillo*, 2004; *Sabra et al.*, 2005; *Shapiro et al.*, 2005]. In a diffuse regime the net energy flux is null and this lead to equipartitioned fields. Equipartition means that in the phase space the available energy is equally distributed, with fixed average amounts, among all the possible states. After sufficiently long time, the energy ratios of the modes tend to stabilize to a constant value, independent of the details of the scattering [see *Ryzhik et al.*, 1996]. The ratio of *S* and *P* energies in the equipartition regime for the full elastic space in 2D and 3D has been obtained by *Weaver* [1982].

[4] Dealing with a diffuse field in open heterogeneous systems *Wapenaar* [2004] and *Weaver and Lobkis* [2004] independently established similar identities between the Green function and correlations of the diffuse field. The Green function that emerges from the correlations is the full, complete Green function of the medium, symmetrized in time, having all reflections, and the scattering and all propagation modes. These derivations imply a great generality. Despite this, their authors gave quite distinct interpretations. While *Weaver and Lobkis* [2004] favor a diffuse wavefield illumination, *Wapenaar* [2004] considers multiple independent, uncorrelated sources. These interpretations have to be reconciled. The results and theoretical developments due to *van Manen et al.* [2005, 2006] can be useful to this aim. These authors considered finite difference modeling and inversion of wave propagation in inhomogeneous media and used a correlation type representation theorem to express the Green function between interior points in terms of Green functions for both displacements and tractions at a boundary. Their representation theorem, a "perfect time reversal device" is a deterministic construct and can be used to connect both approaches. To delve into these interpretations is fascinating but beyond the scope of this letter.

[5] What concerns us is to understand the inner clockwork mechanism that controls this phenomenon. There are few things more useful than a perfect analytical solution. A canonical problem (from Greek κανών = rule, law, standard) is a perfect example. Like Sommerfeld's solution for the diffraction of a scalar wave by a half plane (a landmark of perfection), analytical solutions could help understanding and be useful to clarify interpretations.

[6] In this letter we deal with the canonical problem of an inhomogeneous elastic medium with a 2D cylindrical elastic inclusion subjected to an isotropic random distribution of waves. The cross-correlation of the fields produced at two points by generic plane waves is computed, and then azimuthally averaged. We show that the Fourier transform of the average of the cross-correlation of the vector motion between two points is proportional to the imaginary part of the Green tensor between these points. Moreover, in the *P-SV* case the energy densities for *S* and *P* waves (E_S, E_P, respectively) must satisfy the relationship $E_S/E_P = (\alpha/\beta)^2$, where α, β = wave propagation velocities. This energy ratio is the one predicted by equipartition in the full space. These

[1] Instituto de Ingeniería, Universidad Nacional Autónoma de México, Coyoacán, Mexico.
[2] Departamento de Física Aplicada, Universidad de Almería, Almería, Spain.
[3] Laboratoire de Geophysique Interne et Tectonophysique, Observatoire de Grenoble, Université Joseph Fourier, Grenoble, France.

0094-8276/06/2006GL026454

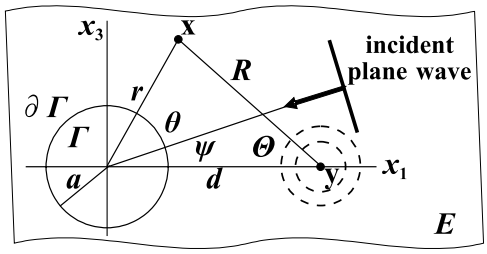

Figure 1. Configuration for the elastic circular cylinder within an infinite space. Receivers are located at **y** and **x**. An incoming plane wave is depicted.

results confirm our previous findings for an infinite homogeneous elastic medium [see *Sánchez-Sesma and Campillo*, 2006].

[7] We used the same approach and obtained precisely the same result when there is a cylindrical inclusion of arbitrary properties. Again isotropy and equipartition of the background field are necessary conditions to retrieve the *exact* Green function from correlations. The equipartition of the background field, regardless the presence of the inclusion is remarkable. This is not at all obvious at first look in abstract representation theorems.

2. Two-Dimensional Scalar Case With a Cylindrical Inclusion

[8] Without loss of generality we assume *SH* waves in a homogeneous elastic medium [see, e.g., *Aki and Richards*, 1980]. Propagation takes place in the x_1–x_3 plane. Therefore, the antiplane (out-of-plane) displacement $v(\mathbf{x}, t)$ fulfils the wave equation

$$\frac{\partial^2 v}{\partial x_1^2}+\frac{\partial^2 v}{\partial x_3^2}=\frac{1}{\beta^2}\frac{\partial^2 v}{\partial t^2}, \tag{1}$$

where β = shear wave velocity and t = time. The 2D Green function for points **x** and **y** is:

$$G_{22}(x_1,x_3,y_1,y_3;\omega)=\frac{1}{4i\mu}H_0^{(2)}(kR), \tag{2}$$

where $\mathbf{x}^T = (x_1, x_3)$, $\mathbf{y}^T = (y_1, y_3)$, $R=\sqrt{(x_1-y_1)^2+(x_3-y_3)^2}$, μ = shear modulus, k = ω/β = shear wavenumber, $i=\sqrt{-1}$, and $H_0^{(2)}(\bullet)$ = Hankel function of the second kind and zero order. Assume now the presence of a cylindrical inclusion of radius a centered at the origin. Equation (2) will be specialized to be the displacement field produced by a unit harmonic line load at $y_1 = d$, $y_3 = 0$. Let's call **y** the source point (see Figure 1). The displacement is calculated at point **x**, which is at a distance r from the origin in the azimuth θ with respect to x_1-axis. When the Graf's addition theorem [see *Abramowitz and Stegun*, 1972] is applied it is possible to express the Hankel function as

$$H_0^{(2)}(kR)=\sum_{n=0}^{\infty}\varepsilon_n J_n(kr_<)H_n^{(2)}(kr_>)\cos(n\theta), \tag{3}$$

where ε_n = Neumann factor(= 1 if $n = 0$, = 2 for $n > 0$), $J_n(\bullet)$ = Bessel function of the first kind and order n, $r_<$ = $\min(d, r)$, and $r_>$ = $\max(d, r)$.

[9] The total motion is the superposition of the free field and the so-called scattered or diffracted waves by the inclusion. In this way it is possible to write the field as the sum of incident and diffracted waves:

$$G_{22}(\mathbf{x},\mathbf{y};\omega)=v^0+v^d=\frac{1}{4i\mu}\left\{H_0^{(2)}(kR)+\sum_{n=0}^{\infty}\varepsilon_n A_n H_n^{(2)}(kd)H_n^{(2)}(kr)\cos n\theta\right\}. \tag{4}$$

[10] The coefficients A_n of the expansion of the diffracted field are obtained from boundary conditions of continuity of both displacements and tractions at the boundary $\partial\Gamma$ of the inclusion. One can find

$$A_n=-\frac{J_n(ka)J_n'(qa)-\xi J_n'(ka)J_n(qa)}{H_n^{(2)}(ka)J_n'(qa)-\xi H_n^{(2)\prime}(ka)J_n(qa)}. \tag{5}$$

These are the coefficients for the radiated waves. Here $\xi=\frac{\mu_E k}{\mu_\Gamma q}=\frac{\rho_E\beta_E}{\rho_\Gamma\beta_\Gamma}$, ($\mu_E$, ρ_E, k) and (μ_Γ, ρ_Γ, q) are shear moduli, mass densities and shear wavenumbers for the exterior medium and the inclusion, respectively. Notice that if $\xi \to \infty$ we recover the cavity coefficients. At this point, the analytical Green function for a medium with a cylindrical inclusion for the 2D scalar case has been obtained.

[11] We calculate further the cross-correlation of the motion in both points **x** and **y**, due to the incidence of *SH* plane waves from all possible incidence angles. Our aim is to show we can retrieve the previously derived Green function from averaging correlations.

[12] A harmonic, homogeneous plane wave can be written as

$$v(\mathbf{x},\omega,t)=F(\omega,\psi)\exp\left(-ikx_jn_j\right)\exp(i\omega t), \tag{6}$$

where $k = \omega/\beta = S$ wavenumber, $F(\omega, \psi)$ = complex waveform, ω = circular frequency, $\mathbf{x}^T$ = Cartesian coordinates (such that $x_1 = r\cos\theta = r\gamma_1$, $x_3 = r\sin\theta = r\gamma_3$, with r, θ = polar coordinates) and n_j = direction cosines ($n_1 = \cos\psi$, $n_3 = \sin\psi$) defining wave propagation. In this way the dot product is $n_j x_j = rn_j\gamma_j = r\cos(\psi - \theta)$. Hereafter time factor $\exp(i\omega t)$ is omitted. Applying the Neumann expansion of exponential it is possible to write,

$$\exp(ikr\cos[\psi-\theta])=\sum_{n=0}^{\infty}\varepsilon_n i^n J_n(kr)\cos n(\psi-\theta) \tag{7}$$

where ε_n = Neumann factor (=1 if $n = 0$, = 2 for $n > 0$). Let us assume $F(\omega, \psi)$ independent of incoming angle ψ to become simply $F(\omega)$. This choice means we assume isotropy of the background radiation. In practice, this condition may not occur and explicit consideration must be paid to azimuthal variations of the field. To this end the methods developed by *Cox* [1973] are in order. It is

convenient to express the motion as the sum of both the incoming (or free) and diffracted fields, which are given by

$$v^0(\mathbf{x},\omega) = F(\omega)\sum_{n=0}^{\infty}\varepsilon_n \mathrm{i}^n J_n(kr)\cos n(\psi-\theta), \tag{8}$$

and

$$v^d(\mathbf{x},\omega) = F(\omega)\sum_{n=0}^{\infty}\varepsilon_n \mathrm{i}^n A_n H_n^{(2)}(kr)\cos n(\psi-\theta). \tag{9}$$

The coefficients A_n are precisely the ones given in equation (5). Then we can express the displacement at the points $\mathbf{x} \equiv (r, \theta)$ by means of the expression:

$$v(r,\theta;\psi) = F(\omega)\sum_{n=0}^{\infty} V_n(r,\omega)\cos n(\theta-\psi), \tag{10}$$

where

$$V_n(r,\omega) = \mathrm{i}^n\varepsilon_n\left[J_n(kr) - A_n H_n^{(2)}(kr)\right], \tag{11}$$

Therefore the cross-correlation can be expressed as

$$v(\mathbf{y},\omega)v^*(\mathbf{x},\omega) = F^2(\omega)\sum_{n=0}^{\infty}\sum_{m=0}^{\infty} V_n(d,\omega) \cdot V_m^*(r,\omega)\cos n\psi\cos m(\psi-\theta) \tag{12}$$

And the azimuthal average over ψ leads to

$$\langle v(\mathbf{y},\omega)v^*(\mathbf{x},\omega)\rangle = F^2(\omega)\sum_{n=0}^{\infty}\sum_{m=0}^{\infty} V_n(d,\omega)V_m^*(r,\omega) \cdot\frac{1}{2\pi}\int_0^{2\pi}\cos n\psi\cos m(\psi-\theta)d\psi. \tag{13}$$

The integral leads to $(1/\varepsilon_n)\delta_{nm}$ (no summation) and thus we have:

$$\langle v(\mathbf{y},\omega)v^*(\mathbf{x},\omega)\rangle = F^2(\omega)\sum_{m=0}^{\infty}\frac{1}{\varepsilon_m}V_m(d,\omega)V_m^*(r,\omega)\cos m\theta. \tag{14}$$

In this equation $F^2(\omega)$ stands for the average spectral density, $E_{SH} = \rho\omega^2F^2(\omega)/2$ is the energy density for *SH* waves. The product of radial functions can be written as:

$$V_m(d,\omega)V_m^*(r,\omega) = \varepsilon_m^2\left(J_m(kd) - A_m H_m^{(2)}(kd)\right) \cdot\left(J_m(kr) - A_m^* H_m^{(1)}(kr)\right). \tag{15}$$

Define $A_n = -N_n/D_n$ with the numerator $N_n = J_n(ka)J_n'(qa) - \xi J_n'(ka)J_n(qa)$, and the denominator $D_n = H_n^{(2)}(ka)J_n'(qa) - \xi H_n^{(2)'}(ka)J_n(qa)$. Therefore, we have

$$\frac{1}{\varepsilon_m}V_m(d,\omega)V_m^*(r,\omega) = \frac{\varepsilon_m}{D_m^2}\left(D_m J_m(kd) - N_m H_m^{(2)}(kd)\right) \cdot\left(D_m J_m(kr) - N_m H_m^{(2)}(kr)\right)^* \tag{16}$$

This expression is real and can be rewritten as

$$\frac{1}{\varepsilon_m}V_m(d,\omega)V_m^*(r,\omega) = \frac{\varepsilon_m}{D_m^2}\left(N_m Y_m(kd) - M_m J_m(kd)\right) \cdot\left(N_m Y_m(kr) - M_m J_m(kr)\right), \tag{17}$$

with $M_n = Y_n(ka)J_n'(qa) - \xi Y_n'(ka)J_n(qa)$. Note that $D_n = N_n - \mathrm{i}M_n$.

[13] Now consider the imaginary part of the Green function in equation (4) which can be written as

$$\begin{aligned}\mathrm{Im}[G_{22}(\mathbf{x},\mathbf{y};\omega)] &= \frac{-1}{4\mu}\Big\{J_0(kR) + \sum_{m=0}^{\infty}\varepsilon_m \cdot\mathrm{Re}\left[A_m H_m^{(2)}(kd)H_m^{(2)}(kr)\right]\cos m\theta\Big\}\\ &= \frac{-1}{4\mu}\sum_{m=0}^{\infty}\varepsilon_m\left\{J_m(kd)J_m(kr) - \mathrm{Re}\left(\frac{N_m}{D_m}H_m^{(2)}(kd)H_m^{(2)}(kr)\right)\right\}\cos m\theta.\end{aligned} \tag{18}$$

Which, after some simplification, can be expressed in the form

$$\mathrm{Im}[G_{22}(\mathbf{x},\mathbf{y};\omega)] = \frac{-1}{4\mu}\sum_{m=0}^{\infty}\frac{\varepsilon_m}{D_m^2}\left(N_m Y_m(kd) - M_m J_m(kd)\right) \cdot\left(N_m Y_m(kr) - M_m J_m(kr)\right)\cos m\theta \tag{19}$$

From equations (14), (17) and (19) we can write

$$\langle v(\mathbf{y},\omega)v^*(\mathbf{x},\omega)\rangle = -8E_{SH}k^{-2}\mathrm{Im}[G_{22}(\mathbf{x},\mathbf{y},\omega)], \tag{20}$$

which is the same as in the homogeneous medium [*Sánchez-Sesma and Campillo*, 2006].

3. Two-Dimensional Vector Case

[14] Assume *P* and *SV* waves in a homogeneous, isotropic, elastic medium (see Figure 1). Propagation takes place in the x_1–x_3 plane. Let us remember the form of the Green's function [e.g., *Sánchez-Sesma and Campillo*, 1991]:

$$G_{ij}(\mathbf{x},\mathbf{y}) = \frac{1}{\mathrm{i}8\rho}\left\{A\delta_{ij} - B\left(2\gamma_i\gamma_j - \delta_{ij}\right)\right\}\ i,j = 1,3, \tag{21}$$

where

$$A = \frac{H_0^{(2)}(qr)}{\alpha^2} + \frac{H_0^{(2)}(kr)}{\beta^2}\ \text{and}\ B = \frac{H_2^{(2)}(qr)}{\alpha^2} - \frac{H_2^{(2)}(kr)}{\beta^2}, \tag{22}$$

with $H_m^{(2)}(\bullet) = J_m(\bullet) - \mathrm{i}Y_m(\bullet)$ = Hankel function of the second kind and order m expressed in terms of the Bessel functions of the first and second kind. The *S* and *P* wavenumbers are given by $k = \omega/\beta$ and $q = \omega/\alpha$, respectively.

[15] In order to solve the problem for a cylindrical inclusion it is necessary to obtain the tensor Green function in polar coordinates using Graf's addition theorem to obtain the incident waves from a line force away from the origin in the reference system of the inclusion. Then the scattered and

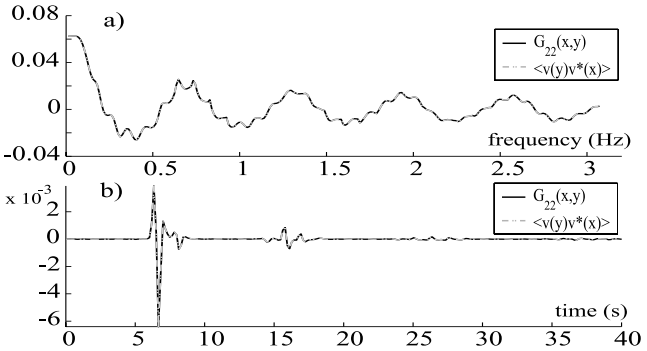

Figure 2. (a) Solid black line depicts the imaginary part of the Green function. The dashed gray line is the average cross-correlation between the displacements recorded at points **x** and **y**. (b) The solid black line is the synthetic seismogram generated by the analytical Green function. The dashed gray line represents the synthetic seismogram generated by the cross-correlation and its Hilbert transform.

refracted elastic waves are computed using the classical coefficients by *Pao and Mow* [1973]. For a recent revision and validation see [*Mercerat et al.*, 2006]. Similarly, the illumination is provided by incoming plane *P* and *SV* waves which are expanded in cylindrical coordinates and the corresponding scattered and refracted fields are obtained. Expressions for the cross-correlations are then obtained and the azimuthal average is done analytically. The development of both tensor quantities, the Green function and the cross-correlations, parallel the case *SH* but with much more complexity because polar coordinates have to be used. Moreover, care must be exercised because the symmetry that holds in the homogeneous case is no longer valid. The final expressions will be reported elsewhere. What is of interest now is the result. If $E_S/E_P = \alpha^2/\beta^2$ we can write

$$\langle u_i(\mathbf{y},\omega)u_j^*(\mathbf{x},\omega)\rangle = -8E_S k^{-2}\mathrm{Im}\left[G_{ij}(\mathbf{x},\mathbf{y},\omega)\right] \qquad (23)$$

Here $E_S = \rho\omega^2 S^2/2$ and $E_P = \rho\omega^2 P^2/2$. The result is the extension of the *SH* case given in equation (20) and is also identical to the result reported by *Sánchez-Sesma and Campillo* [2006] for the 2D vector case in a homogeneous space.

4. Numerical Examples

[16] Two models are considered. First an antiplane *SH* case is studied. With reference to Figure 1, we assumed an elastic space, the exterior region *E*, with *S*-wave velocity $\beta_E = 2$ km/s with a cylindrical inclusion of radius $a = 2$ km and velocity $\beta_\Gamma = 1$ km/s. Mass densities are equal. The receiver is placed at the point **x** while the unit line force is located at **y**. The point **y** is at distance $d = 6$ km to the origin with azimuth zero. For receiver **x** we have $r = 4$ km and $\theta = 30$ degrees. In Figure 2a the imaginary part of $G_{22}(\mathbf{x}, \mathbf{y}, \omega)$ and the average cross-correlation between the displacements at both receivers are displayed against frequency. Calculations were done for 256 frequencies up to 3.2 Hz and the number of terms in the wave functions expansions varies linearly with frequency from 15 to 80 terms. One can observe excellent agreement of these traces. The effects of the heterogeneity are clearly visible in the faint oscillations of Im[G_{22}] which reveals the resonances of the energy trapped within the inclusion.

[17] In Figure 2b we display synthetic seismograms. They are computed from convolving a Ricker wavelet (with characteristic period $t_p = 0.75s$) with both the analytic Green function and the real part of the cross-correlation, respectively. We can observe a very good agreement between both synthetics. We have used the Hilbert transform to generate the real part of the retrieved Green function obtained from the average of cross-correlation (which is the imaginary part).

[18] For the *P-SV* inplane problem the computations are done numerically over the analytical expressions. Considering Figure 1, we assumed a zone *E* with *S*-wave velocity $\beta_E = 0.6$ km/s, *P*-wave velocity $\alpha_E = 1.0$ km/s and density $\rho_E = 2.4$ g/cm^3, while the cylindrical inclusion Γ has a radius $a = 0.25$ km and *S*-wave velocity $\beta_\Gamma = 0.4$ km/s, *P*-wave velocity $\alpha_\Gamma = 0.8$ km/s and mass density $\rho_\Gamma = 2.1$ g/cm^3. Two receivers are placed in this model at the points **x** and **y**. The point **y** is separated a distance $d = 1.05$ km from the origin with zero azimuth. The point **x** is placed at $r = 1.0$ km and $\theta = 135$ degrees. In Figure 3a the imaginary part of the four components of the tensor Green function are presented together with the real part of the average cross-correlation of the suitable displacements recorded at both receivers. An excellent agreement is observed.

[19] Figure 3b displays synthetic seismograms. We convolved a Ricker wavelet (with characteristic period $t_p = 0.6s$) with the analytic Green tensor and the cross-correlations, respectively. Again we used the Hilbert transform to generate the real parts of the tensor Green function which comes from the average of cross-correlations. For verification purposes we added the waveforms computed with finite differences [see *Pérez-Ruiz et al.*, 2005] and we found that the agreement is excellent.

[20] These results for the Green tensor show the soundness of our approach. For an unbounded elastic space it is well-known that the Green function $G_{ij}(\mathbf{x}, \mathbf{y})$ is a symmetric tensor. However, the elastodynamic Green tensor for a heterogeneous medium or for a homogeneous body with boundaries is no longer symmetric. In fact, for our heterogeneous problem we have verified that $G_{ij}(\mathbf{x}, \mathbf{y}, \omega) \neq G_{ji}(\mathbf{x}, \mathbf{y}, \omega)$ and $G_{ij}(\mathbf{x}, \mathbf{y}, \omega) \equiv G_{ji}(\mathbf{y}, \mathbf{x}, \omega)$, for $i \neq j$. This is a consequence of reciprocity.

5. Conclusions

[21] The retrieval of 2D heterogeneous Green function of an elastic cylindrical inclusion embedded in an infinite homogeneous, elastic medium which is illuminated by isotropic random wavefield that fulfills the equipartition ratio characteristic of the full space (in the *P-SV* case) is an important canonical problem. This equipartition of the energy carried by diffuse elastic waves in 2D is given by the relationship $E_S = (\alpha/\beta)^2 E_P$, where E_S and E_P are the S and P spatial energy densities, and α and β are the *P* and *S* wave speeds, respectively.

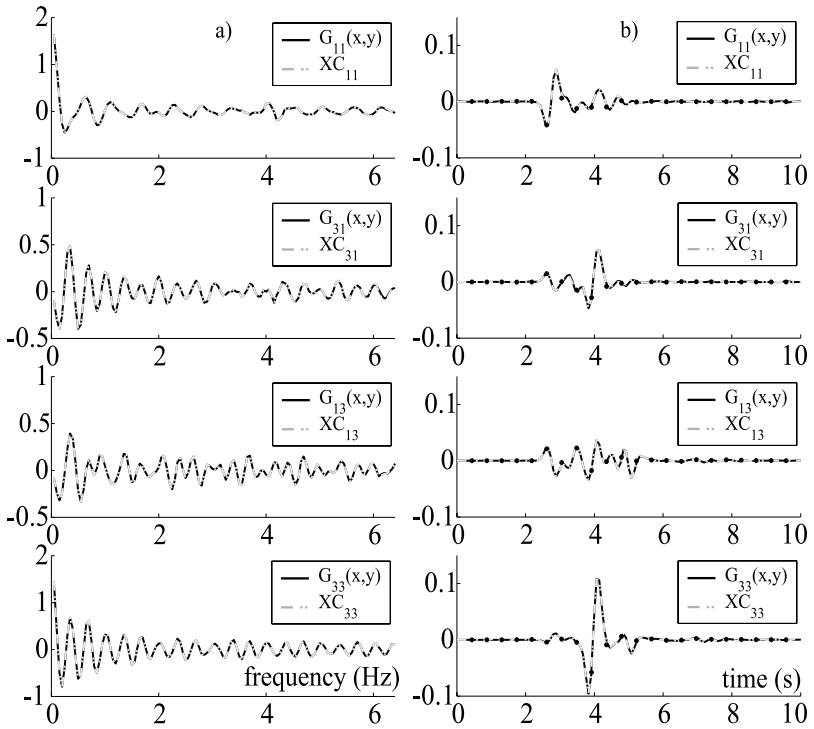

Figure 3. (a) Solid black lines depict the imaginary parts of the tensor Green function. The dashed gray lines are the average cross-correlations between the displacements recorded at points **x** and **y**. (b) The solid traces are the synthetic seismograms from the analytical Green function while dashed gray lines depicts the synthetic seismogram from cross-correlations and their Hilbert transforms. Dots represent Finite Differences solution.

[22] The results presented here for a cylindrical inclusion are the solution for a canonical problem and show beyond doubts that for this simple composite medium we retrieve, from the correlations of the field produced by the isotropic and equipartitioned elastic background, the exact Green function. This is in agreement with theoretical results and reveals the internal, exquisite, mechanism behind this phenomenon. These results will be useful to do the necessary fine tuning to the theory and to compute more realistic problems. Anisotropic background radiation and the effects of attenuation are problems that deserve further scrutiny.

[23] Note that the usefulness of correlations is not confined to the retrieval of the Green function. Indeed, correlations do provide significant, useful information even in cases where the diffuse nature of the fields is not at all obvious. A significant implication of the present results is that being the cylindrical inclusion embedded in a full space the equipartitioned, isotropic illumination (a background radiation) is independent of the scatterer but the local equipartitioned regime already includes its effects.

[24] **Acknowledgments.** We acknowledge the comments from E. Kausel, H. Sato and R. L. Weaver. Thanks are given to A. García-Jerez for the careful reading of the manuscript and his constructive remarks. Partial supports from CONACYT, Mexico, under grant NC-204; from DGAPA-UNAM, Mexico, under grant IN114706; from project DyETI of INSU-CNRS, France; from project CGL2005-05500-C02-02/BTE from CICYT, Spain; from the EU with FEDER; and the Research Team RNM-194 of Junta de Andalucía, Spain, are gratefully acknowledged.

References

Abramowitz, M., and I. A. Stegun (1972), *Handbook of Mathematical Functions*, Dover, Mineola, N. Y.

Aki, K. (1957), Space and time spectra of stationary stochastic waves with special reference to microtremors, *Bull. Earthquake Res. Inst.*, *35*, 415–456.

Aki, K., and P. G. Richards (1980), *Quantitative Seismology*, W. H. Freeman, New York.

Campillo, M., and A. Paul (2003), Long range correlations in the seismic coda, *Science*, *299*, 547–549.

Cox, H. (1973), Spatial correlation in arbitrary noise fields with applications to ambient sea noise, *J. Acoust. Soc. Am.*, *54*, 1289–1301.

Mercerat, E. D., J.-P. Vilotte, and F. J. Sánchez-Sesma (2006), Triangular spectral element simulation of 2D elastic wave propagation using unstructured triangular grids, *Geophys. J. Int.*, in press.

Pao, Y.-H., and C.-C. Mow (1973), *Diffraction of Elastic Waves and Dynamics Stress Concentrations*, Crane Russak/Adam Hilger, New York.

Pérez-Ruiz, J. A., F. Luzón, and A. García-Jerez (2005), Simulation of an irregular free surface with a displacement finite difference scheme, *Bull. Seismol. Soc. Am.*, *95*, 2216–2231.

Ryzhik, L. V., G. C. Papanicolau, and J. B. Keller (1996), Transport equations for elastic and other waves in random media, *Wave Motion*, *24*, 327–370.

Sabra, K. G., P. Gerstoft, P. Roux, W. A. Kuperman, and M. C. Fehler (2005), Extracting time-domain Green's function estimates from ambient seismic noise, *Geophys. Res. Lett.*, *32*, L03310, doi:10.1029/2004GL021862.

Sánchez-Sesma, F. J., and M. Campillo (1991), Diffraction of *P, SV* and Rayleigh waves by topographic features: A boundary integral formulation, *Bull. Seismol. Soc. Am.*, *81*, 2234–2253.

Sánchez-Sesma, F. J., and M. Campillo (2006), Retrieval of the Green function from cross-correlation: The canonical elastic problem, *Bull. Seismol. Soc. Am.*, *96*, 1182–1191.

Sato, H., and M. Fehler (1998), *Wave Propagation and Scattering in the Heterogeneous Earth*, Springer, New York.

Shapiro, N. M., and M. Campillo (2004), Emergence of broadband Rayleigh waves from correlations of the ambient seismic noise, *Geophys. Res. Lett.*, *31*, L07614, doi:10.1029/2004GL019491.

Shapiro, N. M., M. Campillo, L. Stehly, and M. Ritzwoller (2005), High resolution surface wave tomography from ambient seismic noise, *Science*, *307*, 1615–1618.

van Manen, D.-J., J. O. A. Robertsson, and A. Curtis (2005), Modeling of wave propagation in inhomogeneous media, *Phys. Rev. Lett.*, *94*, 164301.

van Manen, D.-J., A. Curtis, and J. O. A. Robertsson (2006), Interferometric modelling of wave propagation in inhomogeneous elastic media using time-reversal and reciprocity, *Geophysics*, in press.

Wapenaar, K. (2004), Retrieving the elastodynamic Green's function of an arbitrary inhomogeneous medium by cross correlation, *Phys. Rev. Lett.*, *93*, 254301.

Weaver, R. L. (1982), On diffuse waves in solid media, *J. Acoust. Soc. Am.*, *71*, 1608–1609.

Weaver, R. L., and O. I. Lobkis (2004), Diffuse fields in open systems and the emergence of the Green's function, *J. Acoust. Soc. Am.*, *116*, 2731–2734.

M. Campillo, Laboratoire de Geophysique Interne et Tectonophysique, Observatoire de Grenoble, Université Joseph Fourier, BP 53, F-38041 Grenoble Cedex, France.

F. Luzón and J. A. Pérez-Ruiz, Departamento de Física Aplicada, Universidad de Almería, Cañada de San Urbano s/n, E-04120 Almería, Spain. (fluzon@ual.es)

F. J. Sánchez-Sesma, Instituto de Ingeniería, Universidad Nacional Autónoma de México, Cd. Universitaria, Circuito Escolar s/n, Coyoacán 04510, México D. F., Mexico.